TISSUE ENGINEERING: Part A
Volume 00, Number 00, 2014

DOI: 10.1089/ten.tea.2013.0460

Original Article

Human Skin Cell Fractions Fail to Self-Organize Within a Gellan Gum/Hyaluronic Acid Matrix but Positively Influence Early Wound Healing

Mariana T. Cerqueira, PhD,[1,2] Lucília P. da Silva, MSC,[1,2] Tírcia C. Santos, PhD,[1,2] Rogério P. Pirraco, PhD,[1,2] Vitor M. Correlo, PhD,[1,2] Alexandra P. Marques, PhD,[1,2] and Rui L. Reis, PhD[1,2]

Split-thickness autografts still are the current gold standard to treat skin, upon severe injuries. Nonetheless, autografts are dependent on donor site availability and often associated to poor quality neoskin. The generation of dermal–epidermal substitutes by tissue engineering is seen as a promising strategy to overcome this problematic. However, solutions that can be safely and conveniently transplanted in one single surgical intervention are still very challenging as their production normally requires long culture time, and graft survival is many times compromised by delayed vascularization upon transplantation. This work intended to propose a strategy that circumvents the prolonged and laborious preparation period of skin substitutes and allows skin cells self-organization toward improved healing. Human dermal/epidermal cell fractions were entrapped directly from isolation within a gellan gum/hyaluronic acid (GG-HA) spongy-like hydrogel formed from an off-the-shelf dried polymeric network. Upon transplantation into full-thickness mice wounds, the proposed constructs accelerated the wound closure rate and re-epithelialization, as well as tissue neovascularization. A synergistic effect of the GG-HA matrix and the transplanted cells over those processes was demonstrated at early time points. Despite the human-derived and chimeric blood vessels found, the proposed matrix did not succeed in prolonging cells residence time and in sustaining the self-organization of transplanted human cells possibly due to primitive degradation. Despite this, the herein proposed approach open the opportunity to tackle wound healing at early stages contributing to re-epithelialization and neovascularization.

Introduction

Despite the wide range of commercially available skin substitutes,[1–4] along with the effort to generate new skin tissue-engineered solutions,[5–7] split-thickness autografts remain the gold standard for skin replacement.[8,9] These autologous skin grafts, combining epidermis but only part of the dermis, are however dependent on donor site availability requiring several surgeries,[10] are associated to some pain and discomfort due to tissue harvesting,[8] and frequently lead to hypertrophic scarring[11] or keloid formation.[12]

It is believed that improved quality neoskin can be achieved using tissue-engineered autologous dermal–epidermal substitutes, which can be securely and conveniently transplanted with minimal scarring in a single surgical intervention. However, artificial skin models that completely replicate normal and uninjured skin are yet to be developed, and only few off-the-shelf bilayered dermal–epidermal substitutes have been engineered.[3] Additionally, despite the complex and rather sophisticated alternatives to design and develop improved dermal–epidermal substitutes, a key question relying on the importance of having a full-differentiated model has recently emerged.[13] Is the mimicking of skin complex structure *in vitro* necessary or is a substitute with minimum level of differentiation and organization that would be more rapidly produced and yet capable of inducing an active and efficient regeneration *in vivo* sufficient? Considering inherent costs and time of production, tissue-engineered constructs with the exact biomimicry of adult skin and a defined extent of differentiation are likely to encompass limited clinical usefulness. Sun *et al.*[14] demonstrated that human skin cells have the ability to self-organize *in vitro* within a three-dimensional (3D) environment deprived from any biochemical cues, underestimating the necessity of having a cellular preorganization within a scaffold for skin tissue engineering. Moreover, Lee *et al.*[13] explored the concept of using dissociated mouse epidermal and dermal cells, demonstrating their ability to interact and self-organize exhibiting a typical topological organization with additional formation of a high number of hair follicles. The

[1]3B's Research Group—Biomaterials, Biodegradables and Biomimetics, University of Minho, Headquarters of the European Institute of Excellence on Tissue Engineering and Regenerative Medicine, Guimarães, Portugal.
[2]ICVS/3B's—PT Government Associate Laboratory, Braga/Guimarães, Portugal.

importance of paracrine cues between the different cell types is highlighted,[14] in agreement with previous works that showed the cross talk between fibroblasts and keratinocytes to be essential to attain a functional skin substitute[15,16] and mesenchymal–epidermal interactions crucial for hair follicle formation.[17]

Minimizing the time of preparation of skin substitutes *in vitro*, reducing production/maintenance costs, adds to the challenge of efficient *in situ* cell delivery with high cell survival percentage. Numerous polymeric matrices derived from both natural[2,18] and synthetic[19–21] sources have been used as cellular supports; nonetheless, the particular need to avoid skin contraction during the regeneration process places a significant role over the properties of that scaffolding matrix. Currently developed matrices intend to be less a simple carrier for cell delivery, and more and more ECM analogues that would help in the remodeling process leading to satisfactory skin regeneration. In this context, hydrogels, due to their hygroscopic nature and soft tissue-like mechanical performance, have been proposed for wound healing applications.[22–25] However, hydrogels lack natural cell adhesion sites[26] and hamper the maximization of their potential for cell niche recreation.

This work proposes a cell-adhesive gellan gum (GG) and hyaluronic acid (HA) spongy-like hydrogel,[27] entrapping dissociated human epidermal and dermal cellular fractions, as a dermal–epidermal substitute to target full-thickness excisional wound regeneration. We hypothesized that the isolated cellular fractions include early differentiation stage keratinocytes, fibroblasts, and endothelial cells, which, together with the proposed biomatrix, would be capable to survive and self-organize to improve neovascularization and to promote a rapid re-epithelialization. Overall, our approach offers the combination of an off-the-shelf matrix with a short time culture of cellular derivatives as an alternative to skin 3D dermal–epidermal substitutes that need fastidious and complex cell isolation procedures, as well as extensive *in vitro* cell culture periods to be generated.

Materials and Methods

Spongy-like hydrogels preparation

GG-HA spongy-like hydrogels were prepared as described previously.[27] In brief, a 0.75% (m/V) hyaluronate (1.5 MDa; LifeCore Biomedical) and 1.25% (m/V) gelzan (Sigma-Aldrich) solution was prepared at 90°C and casted onto 24-well plates. Cross-linking was performed with the addition of divalent cations, such as Ca^{2+},[28] and the hydrogels formed were left to fully hydrate in a phosphate-buffered saline (PBS; Sigma) solution for 48 h. Following that, hydrogels were frozen overnight at −80°C and freeze-dried (Telstar) for 3 days to obtain the dried polymeric networks. Spongy-like hydrogels were achieved by hydration of dried polymeric structures with the culture medium at the time of cell seeding.

Cellular fractions isolation

Epidermal and dermal cellular fractions were isolated from human skin samples, obtained from the Hospital da Prelada (Porto, Portugal), after patient's informed consent and under a collaboration protocol with 3B's Research Group approved by the ethical committees of both institutions. After washing with PBS, skin specimens were cut into small fragments and incubated overnight in Dispase (2.4 μ/mL; BD Biosciences) at 4°C. Epidermis was then peeled off and kept in PBS at 4°C, whereas dermis was digested with 0.1% collagenase type I (Sigma) for 3 h at 37°C under agitation. After that, dermal cellular fraction was obtained through the mechanical dissociation of the enzymatically digested dermis that was then filtered through a sterile 100-μm cell strainer (BD Biosciences), centrifuged, and resuspended in the Endothelial Growth Medium (EGM2; Lonza). Likewise, epidermal cellular fraction was isolated through enzymatic digestion of the epidermis at 37°C for 10 min using 0.05% Trypsin-EDTA (Invitrogen). Digested epidermis was then filtered through a sterile 100-μm cell strainer, centrifuged, and finally resuspended in the keratinocyte serum-free medium (KSFM) (Invitrogen) with 1% Antibiotic/Antimycotic (Invitrogen).

Constructs preparation

To prepare GG-HA spongy-like hydrogel constructs, a ratio of 1:5 epidermal:dermal cellular fractions was used, as previously suggested.[13] Briefly, a combined suspension of 2.5×10^6/mL epidermal and 1.25×10^7/mL dermal cells was prepared, and 100 μL was added to the GG-HA dried network structures (1.2 cm of diameter and 0.3 cm high). Constructs were incubated in a humidified incubator at 37°C and 5% CO_2 for 30 min to enhance cell entrapment. After that time, 2 mL per well of KSFM and EGM2 (1:1) was added, and constructs were cultured *in vitro* for 2 days before *in vivo* implantation. Individual cellular fractions were plated in tissue culture polystyrene (TCPS) coverslips and cultured under the same conditions for 2 days, for parallel cell characterization.

Implantation in mice excisional wounds

In vivo experimental protocol was approved by the Direcção-Geral de Alimentação e Veterinária (DGAV) and the Portuguese National Authority for Animal Health, and all the surgical and necropsy procedures were performed according to the applicable national regulations respecting international animal welfare rules. Twenty-four Swiss Nu/Nu male mice (Charles River Laboratories) were randomly divided in two groups comprising the GG-HA spongy-like hydrogel construct (experimental) and the control where the animals were left with an empty wound (control). Four animals were used per condition and per time point (3, 7, 14, and 21 days). Mice were anesthetized with a mixture of Imalgene (ketamine) (75 mg/kg) (Merial Portuguesa) plus Domitor (medetomidine) (1 mg/kg) (Esteve Farma, LDA). A 1.2-cm-diameter full-thickness excision was performed in each mouse at ~0.5 cm caudal to the intrascapular region. After placing spongy-like hydrogel constructs, wounds were covered with transparent dressing Hydrofilm (Hartmann) and a final set of bandages was used to avoid the dislocation of the transparent dressing and to protect the whole treatment set. Control wounds left empty were dressed likewise. A subcutaneous injection of Depomedrol

(20 mg/kg BW) (Pfizer) was applied to the animals at days 0, 7, and 14 to delay wound healing.[29] The animals were kept separately and at the established endpoints were euthanized by CO_2 inhalation, and explants were processed for histological analysis.

Histology

Skin explants were collected at days 3, 7, 14, and 21 and fixed in 10% formalin (Sigma) and paraffin embedded. Representative sections were stained with routine protocols of hematoxylin and eosin (H&E) and Masson's trichrome. Sections were analyzed with an Axioplan Imager Z1m microscope (Zeiss), and images were acquired and processed with AxioVision V.4.8 software (Zeiss).

Immunolabeling

Immunostaining of both dermal and epidermal cellular fractions in coverslips and in replicates of GG-HA spongy-like hydrogel constructs maintained *in vitro* was performed after fixation with 3.7% (v/v) buffered formalin, permeabilization with 0.2% TritonX-100, and blocking with 3% bovine serum albumin (Sigma). For paraffin-embedded samples, sections were re-hydrated and incubated with Antigen retrieval solution (Tris-EDTA buffer—10 mM Tris Base, 1 mM EDTA solution, 0.05% Tween 20, pH 9.0) (all Sigma) before permeabilization and blocking. Primary antibodies CD31 (mouse anti-human, 1:30; Dako), von Willebrand factor (vWF) (rabbit anti-human/mouse, 1:200; Dako), and keratin 5 (K5) (rabbit anti-human/mouse; Covance), K14 (rabbit-anti-human/mouse, 1:800; Covance), K10 (mouse anti-human/mouse, 1:800; Covance), and CD31 (rabbit anti-human/mice, 1:20; Abcam), and tagged secondary antibodies, rabbit anti-mouse Alexafluor 594 and donkey anti-rabbit Alexafluor 488 (1:500; Invitrogen), were used. For the detection of human/mice CD31, VECTASTAIN Elite ABC Kit (Vector Labs) was used according to the manufacturer's instructions. Nuclei were stained either with DAPI (Invitrogen) or Mayer's hematoxylin. Cytoskeleton F-actin fibers in GG-HA spongy-like hydrogel constructs were stained with Phalloidin-TRITC (Sigma). All the samples were examined under AXIOIMAGER Z1M microscope, using AxioVision software 4.1, with the exception of *in vitro* spongy-like hydrogel constructs that were observed by confocal microscopy, under Olympus Fluoview FV1000.

Chromogenic in situ *hybridization*

Histological sections were deparaffinized, dehydrated, air-dried, and heated in a boiling water bath at 95°C in pretreatment 1% MES buffer (Sigma) for 10 min. Enzymatic digestion was performed using 4 mg/mL pepsin buffer (Worthington) for 40 min at 37°C in a humid chamber. After dehydration, histological slides were air-dried and positive DNA-Biotin-labeled probe (Pan Path) was applied. Denaturation was performed at 95°C for 5 min, and hybridization was achieved at 37°C overnight. After that, samples were incubated for 10 min at 37°C with a stringency wash buffer (Pan Path). Streptavidin–peroxidase complex (Vector Labs) was used for detection, and DAB chromogen substrate system (Vector Labs) was used for revelation. Mayer's hematoxylin was used for counterstaining.

Image analysis

Image analysis for the quantification of wound closure, vessels density, epidermal thickness, and number of hair follicles was performed using Image J image analysis software (Wayne Rasband, NIH) under the conditions detailed in each of the subsections below.

Planimetric digital images were taken on the day of surgery and at days 3, 7, 14, and 21 postimplantation for all four animals, per condition and time point. The percentage of wound closure was then calculated as:

$$\% \text{ of Wound Closure} = \frac{\text{Area of Original Wound} - \text{Area of Actual Wound}}{\text{Area of Original Wound}} \times 100$$

Wound was considered completely closed when the actual wound area was equal to zero.[30]

Vessels density quantification. The number of vessels was quantified at days 7 and 14 postoperative in the CD31-stained samples. Quantification and measurement were performed in randomly selected five high-power fields of five nonconsecutive tissue sections per time point and per animal within each group. Only vessels with a diameter of $< 50\,\mu m$[31] were considered. Mean results of the number of vessels per field are expressed as vessels density.

Epidermal thickness measurement. Epidermal thickness of the formed neoskin was evaluated on H&E-stained histological sections of both the experimental and control groups explanted at day 21. Four tissue sections per animal within each group were analyzed by randomly selecting five high-power fields in each section and performing five measurements of the epidermal thickness per field.

Quantification of hair follicles number. The number of hair follicles formed in the neotissue at day 21 was counted on five randomly selected high-magnification fields of H&E-stained histological sections per animal within the experimental and control groups samples explanted.

Statistic analysis

Four animals ($n = 4$) were used in each group and for each time point. Statistical analysis of wound closure and the number of hair follicles were performed using two-way analysis of variance (ANOVA) with Bonferroni post-tests. Data of vessels density were analyzed by one-way ANOVA with Tukey's post-tests, whereas for epidermal thickness data, statistic analysis was carried out with Kruskal–Wallis test, with Dunn's post-test (GraphPad Prism 4.02). Significance levels, determined using post-tests, between the groups were set at $p < 0.05$.

Results

GG-HA spongy-like hydrogels constructs properties

Cellular fractions used to create the dermal–epidermal constructs were phenotypically analyzed after the culture on TCPS coverslips (Fig. 1A, B) and when entrapped within the GG-HA matrix before *in vivo* transplantation and after 2 days of culture (Fig. 1C, D) to confirm phenotype stability. Cells from the epidermal fraction exhibited homogenous and cuboidal morphology, characteristic of epidermal basal cells. This observation was confirmed by the expression, although at different intensities, of the keratinocytes early differentiation-associated marker, K5, by the cells adhered on the TCPS coverslips (Fig. 1A). Regarding the dermal cellular fraction, in addition to the expected fibroblasts, labeled only with DAPI, endothelial cells, expressing the typical vWF and CD31 markers, were also identified on the TCPS coverslips (Fig. 1B). Endothelial cells displayed their typical cobblestone morphology, and interestingly, despite the co-isolation with other dermal cells, they were capable of rearranging *in vitro*, forming their characteristic colonies (Fig. 1B). After being entrapped in spongy-like hydrogels for 2 days, the cells from the epidermal and dermal fractions also presented the expected phenotypes (Fig. 1C, D). The epidermal cells expressing K5 displayed different morphologies and varied cytoskeleton organization as indicated by the phalloidin staining (Fig. 1C). Moreover, endothelial cells, positive for CD31, also presented a different morphology in comparison to what was observed in TCPS. However, a preferential arrangement of epidermal and endothelial cell-like colonies was observed within the spongy-like hydrogel matrix.

Wound closure

Wound closure was assessed by macroscopic observation along the implantation time (Fig. 2-ii). Wounds showed to be progressively closing along the time, but major differences between the experimental and control groups were identified, significant at earlier time points. Up to day 7 postoperative, wounds with spongy-like hydrogel constructs showed a significantly higher percentage of closure ($p < 0.05$) (Fig. 2-i) than the controls. In the subsequent time points, the experimental group still exhibited slightly higher values, although not statistically significant.

This was confirmed in the macroscopic analysis carried out along the time (Fig. 2-ii); at day 3, the wound treated with spongy-like hydrogel construct exhibited a dim yellowish color, presumably due to the absorption of the cell exudate by the hydrogel, which was not observed in the control group. From day 3 onward, a visible decrease of the wounds size was noticed, more evident in the spongy-like hydrogel-treated group with a nearly complete closure at day 21. Eschar was first distinguished at day 7 in both groups; however, in experimental group, it was absent at day 21, whereas in the control group, a considerable eschar was still present at the endpoint of the assay.

Wound healing progression

The progression of the wound healing was assessed after H&E staining (Fig. 3). Differences between the control and experimental groups revealed that the overall healing process in the experimental group was more accelerated than in the control group.

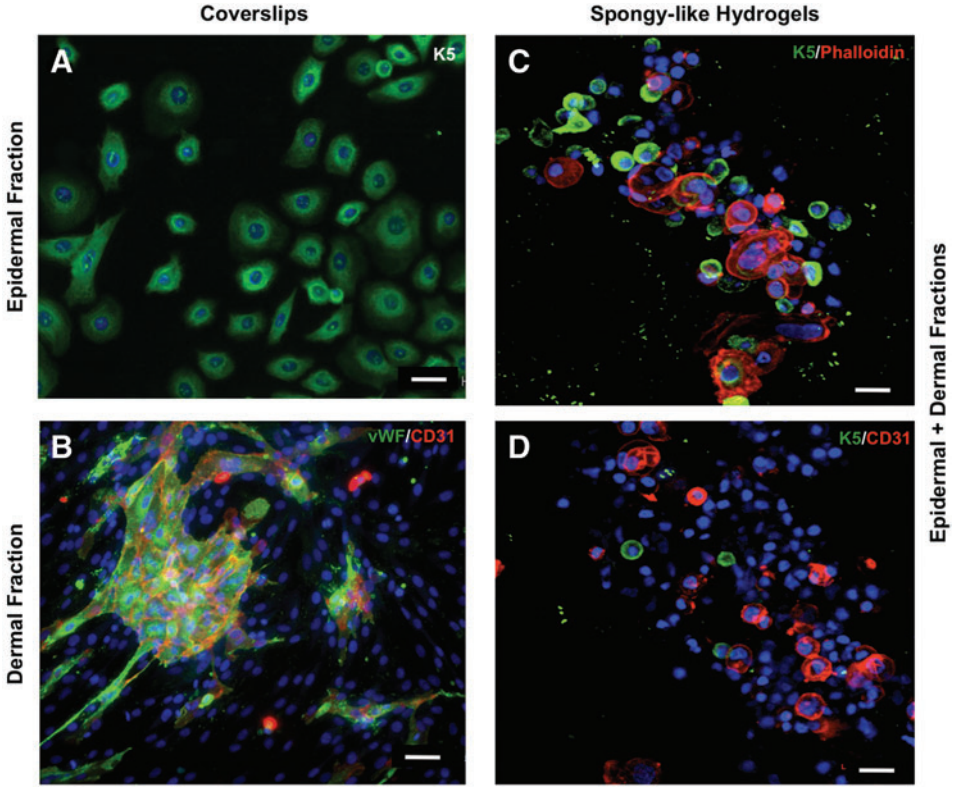

FIG. 1. Phenotypic characterization by immunocytochemistry of cells from the epidermal and dermal fractions after 2 days of culture **(A, B)** on tissue culture polystyrene coverslips and **(C, D)** entrapped in the GG-HA spongy-like hydrogel. **(A, C, D)** Epidermal early-associated marker keratin 5 (K5, green) was expressed by the cells from the epidermal fraction. **(B, D)** Endothelial cells were detected among dermal cellular fraction through the expression of vWF (green) or CD31 (red). Nuclei were stained with DAPI, and cytoskeleton F-actin fibers in GG-HA spongy-like hydrogel constructs were stained with Phalloidin-TRITC. Scale bars correspond to 50 μm. GG-HA, gellan gum/hyaluronic acid; vWF, von Willebrand factor. Color images available online at www.liebertpub.com/tea

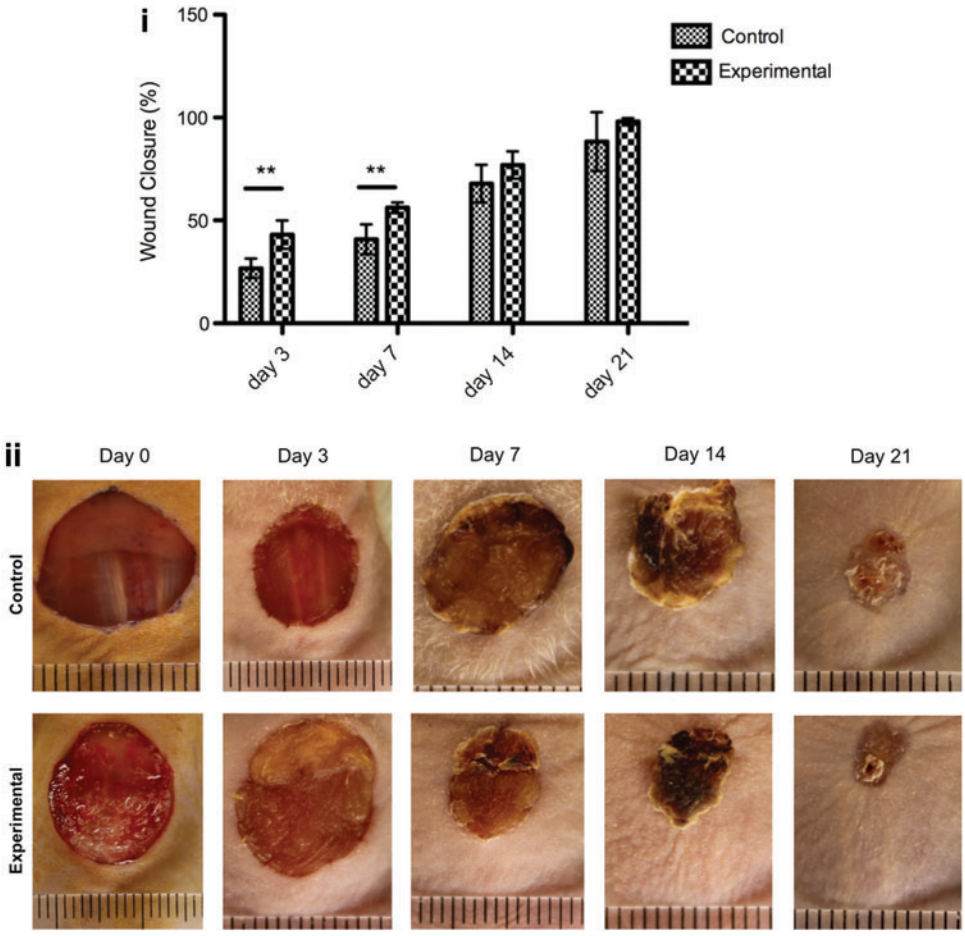

FIG. 2. Evaluation of the effect of spongy-like hydrogel constructs over wound closure. **(i)** Representation of the percentage of wound closure in the experimental and control groups after 3, 7, 14, and 21 days. **(ii)** Representative macroscopic images of the wounds along the implantation time. $^{**}p < 0.01$. Color images available online at www.liebertpub.com/tea

At day 3, granulation tissue formation was almost absent in the control group (Fig. 3A) but was observed in significant amounts in the experimental group (Fig. 3E). In fact, by day 7, granulation tissue was detected in the control group (Fig. 3B), whereas in the experimental group, neoepidermis (Fig. 3F), identified by the expression of K5 (Fig. 4-i, B), was observed underneath the eschar tissue. Similar findings were observed in the control group (Fig. 3C) at day 14, although an exuberant eschar was still present. A complete re-epithelialization of the wounds was observed at day 14 for the experimental group (Fig. 3G) and at day 21 for the control group (Fig. 3D). Nonetheless, epidermal thickness measured at day 21 (Fig. 4E) did not show significant differences between the experimental and control groups.

The immunohistochemical assessment of K5 and K10 expression along the implantation time revealed the presence of K5, but not K10, positive cells both within the spongy-like hydrogel and at the material–wound bed interface 3 days after implantation (Fig. 4-i, A), corresponding to the entrapped human cells from the epidermal fraction (Fig. 5). Moreover, the neoepidermis found in the experimental group after 7 days of implantation was formed by cells strongly expressing K5 in the basal layer, with some cells expressing K10 on the top layers (Fig. 4-i, B). Similar observations were found at day 14 (Fig. 4C), although with a stronger expression of K10. A fully differentiated epidermis and the presence of newly formed hair follicles, expressing characteristic high levels of K5, were identified at day 21 (Fig. 4D). In fact, at day 21, a significantly higher number of hair follicles ($p < 0.05$) were observed in the experimental group compared to the control group (Fig. 4D, F).

The identification of the transplanted human cells from the dermal fraction revealed that while cells expressing fibroblast surface protein were found both within the spongy-like hydrogel and at the material–wound bed interface 3 days after implantation (Fig. 5A, B, E), endothelial cells, positive for CD31, were only present within the hydrogel (Fig. 5A, B, F).

In fact, spongy-like hydrogel constructs promoted a notorious effect on early neovascularization. A significantly higher vessel density ($p < 0.05$) was observed at day 7 for the experimental group in relation to the control group (Fig. 6-i, A), which was not detected at day 14 in which both conditions presented equivalent results regarding the number of vessels in the neotissue (Fig. 6-i, B). At both time points, human endothelial cells were detected within the neoformed vasculature forming both human-derived and chimeric vessels (Fig. 6A–D). Moreover, some of those neovessels were perfused, as observed by the presence of erythrocytes in their lumen (Fig. 6C, D).

Discussion

An effective approach to rapidly cover wounds and actively accelerate healing, shortening the extensive cell culture and respective substitute preparation period, which

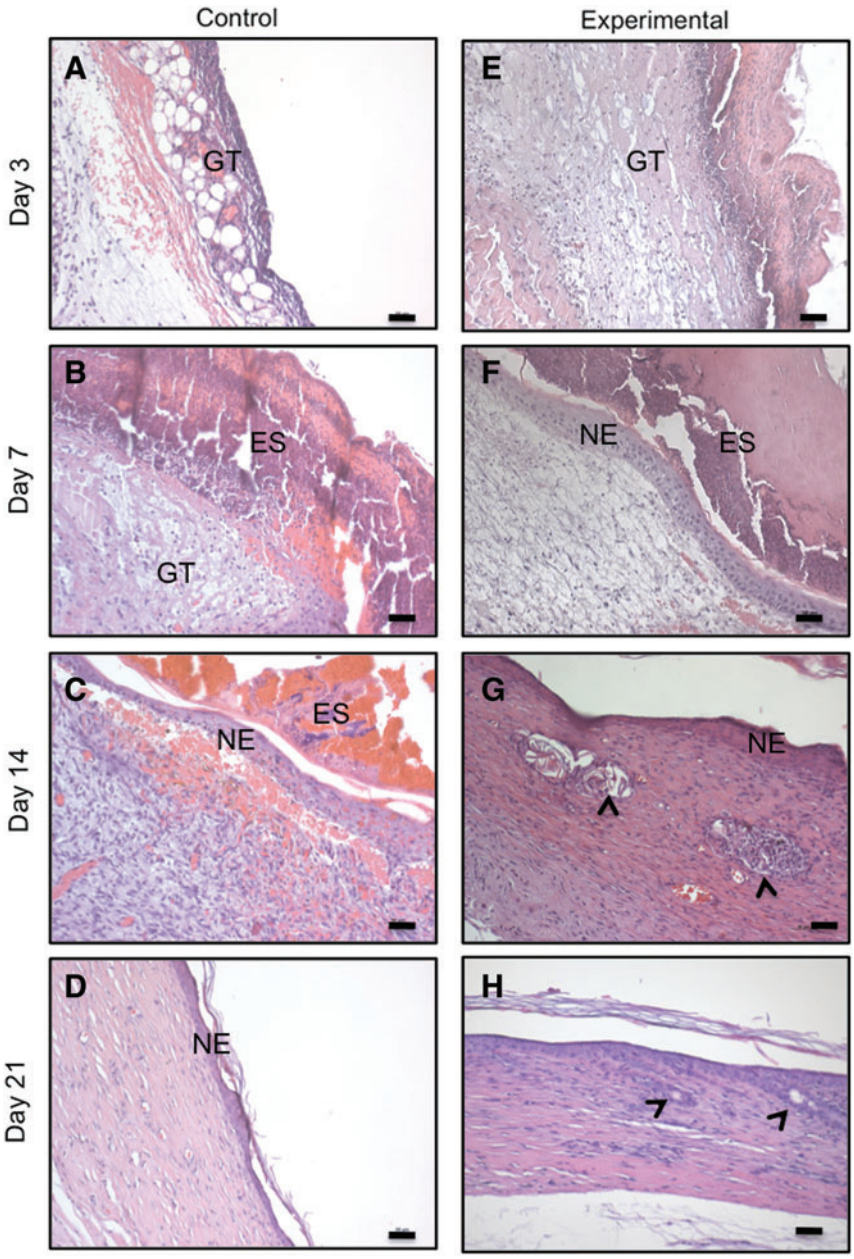

FIG. 3. Representative images of hematoxylin and eosin (H&E)-stained sections of **(A–D)** the control and **(E–H)** experimental group explants, at days 3, 7, 14, and 21 postoperative, revealing the wound healing progression at the centre of the wound. Scale bar corresponds to 50 μm. Arrow heads indicate the hair-follicles formation. GT, granulation tissue; ES, eschar; NE, neoepidermis. Color images available online at www.liebertpub.com/tea

commonly leads to patient complications and decrease of the functionality of implanted cells, still is a major clinical demand.[8] Hence, instead of a full 3D skin biomimetic model, we proposed the use of a 3D system based on a cell-adhesive GG-HA spongy-like hydrogel, as an integrated *in vitro* niche for the self-organization of human epidermal and dermal cellular fractions, used directly from isolation. GG-HA spongy-like hydrogel was chosen, based both on the importance of HA as main skin ECM component, with an active role in skin remodeling,[32,33] and on angiogenesis.[31,34–36] Moreover, spongy-like hydrogels resulted from the hydration of off-the-shelf dried networks at the time of cell seeding, which open the possibility of a ready-to-use application. These spongy-like hydrogels were also shown to be easily manipulated upon transplantation and to possess high ability to shape adaptability, but more importantly, present attractive cell adhesive features that distinguish them from traditional hydrogels.[27] In fact, spongy-like hydrogels have shown to support the adhesion of different cell types, including human keratinocytes, endothelial cells, and fibroblastic cells.[27] Interestingly, the cells obtained from both the epidermal and dermal fractions, and entrapped within the GG-HA spongy-like hydrogel, did not depict the expected morphology after 2 days of culture. This behavior can be related to the fact that cells were entrapped directly from the isolation, without any subculture step that permits the selection of the lineages of interest by adhesion to TCPS under specific culture conditions. Therefore, the cellular fractions directly from the isolation contain other components resultant from the

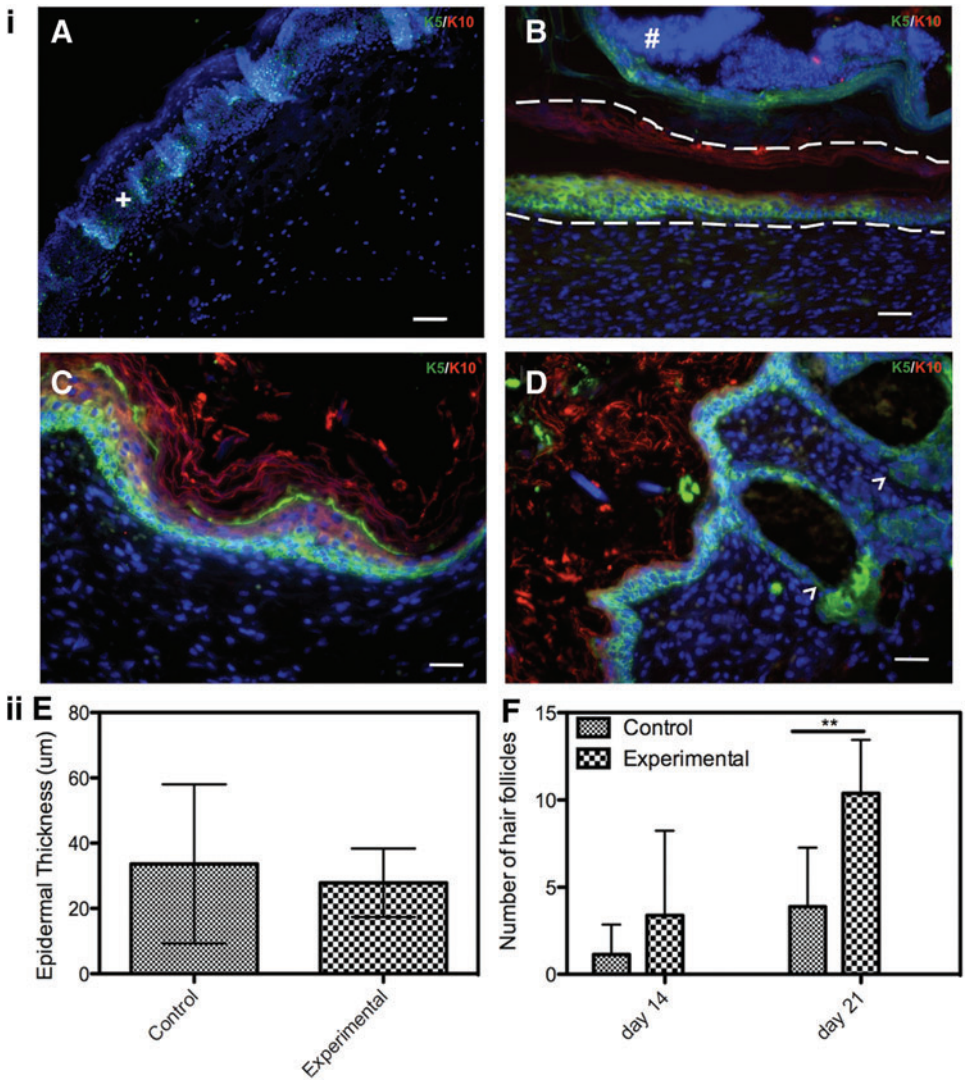

FIG. 4. Epidermal morphogenesis. **(i)** Expression profile of K5 (green) and K10 (red) detected by immunohistochemistry in the experimental group at days **(A)** 3, **(B)** 7, **(C)** 14, and **(D)** 21 postimplantation. **(A)** The presence of K5, but not K10, positive cells within the spongy-like hydrogel (+) 3 days after implantation. **(B)** Early epidermal formation at day 7 (limited by dashed lines) underneath the eschar tissue (#) with **(C–D)** subsequent expression of K10 in suprabasal layers and **(D)** hair follicles formation (arrowheads) at the end of the time point. **(ii)** Analysis of neoepidermis maturation on both the control and experimental groups, based on H&E-stained samples. Representation of **(E)** the epidermal thickness and **(F)** the number of hair follicles at days 14 and 21 postimplantation. $^{**}p < 0.01$. Nuclei were counterstained with DAPI, and scale bars correspond to 50 μm. Color images available online at www.liebertpub.com/tea

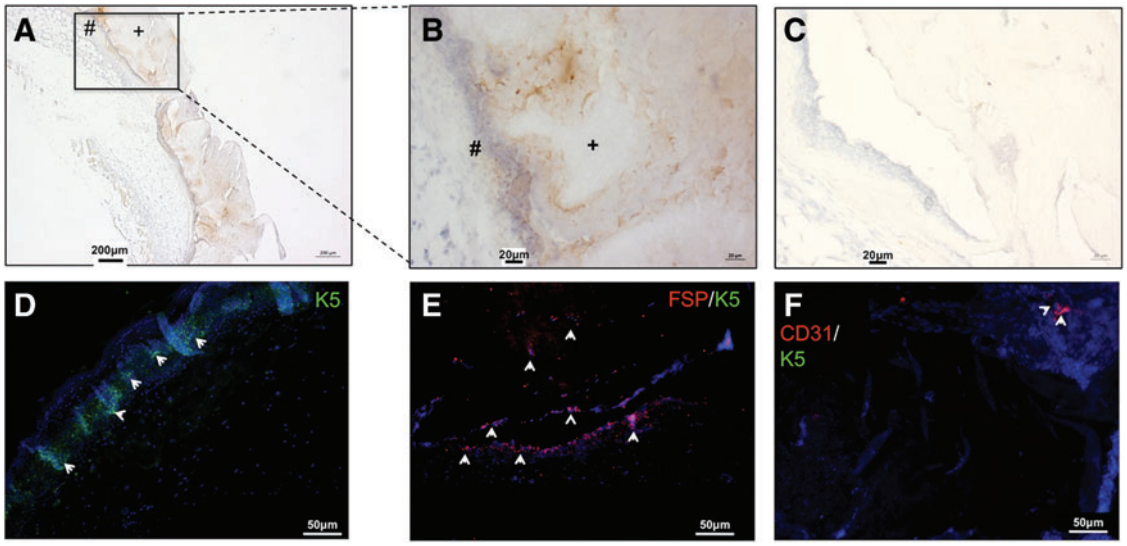

FIG. 5. **(A, B)** Identification of transplanted human cells within spongy-like hydrogel (+) by chromogenic *in situ* hybridization at day 3 postoperative. **(B)** Represents higher magnification of A showing brown nuclei corresponding to human cells both inside the spongy-like hydrogel (+) and in the tissue that is newly forming (#). **(C)** Illustrates the negative control of the assay after hematoxylin counterstaining. **(D–F)** Immunohistochemistry representative images confirming the epidermal (K5-positive cells), endothelial (CD31 expressing cells), and fibroblastic cells positive for fibroblast surface protein (FSP) phenotype of the cells (arrowheads) within the spongy-like hydrogel matrix. Nuclei were stained with DAPI. Color images available online at www.liebertpub.com/tea

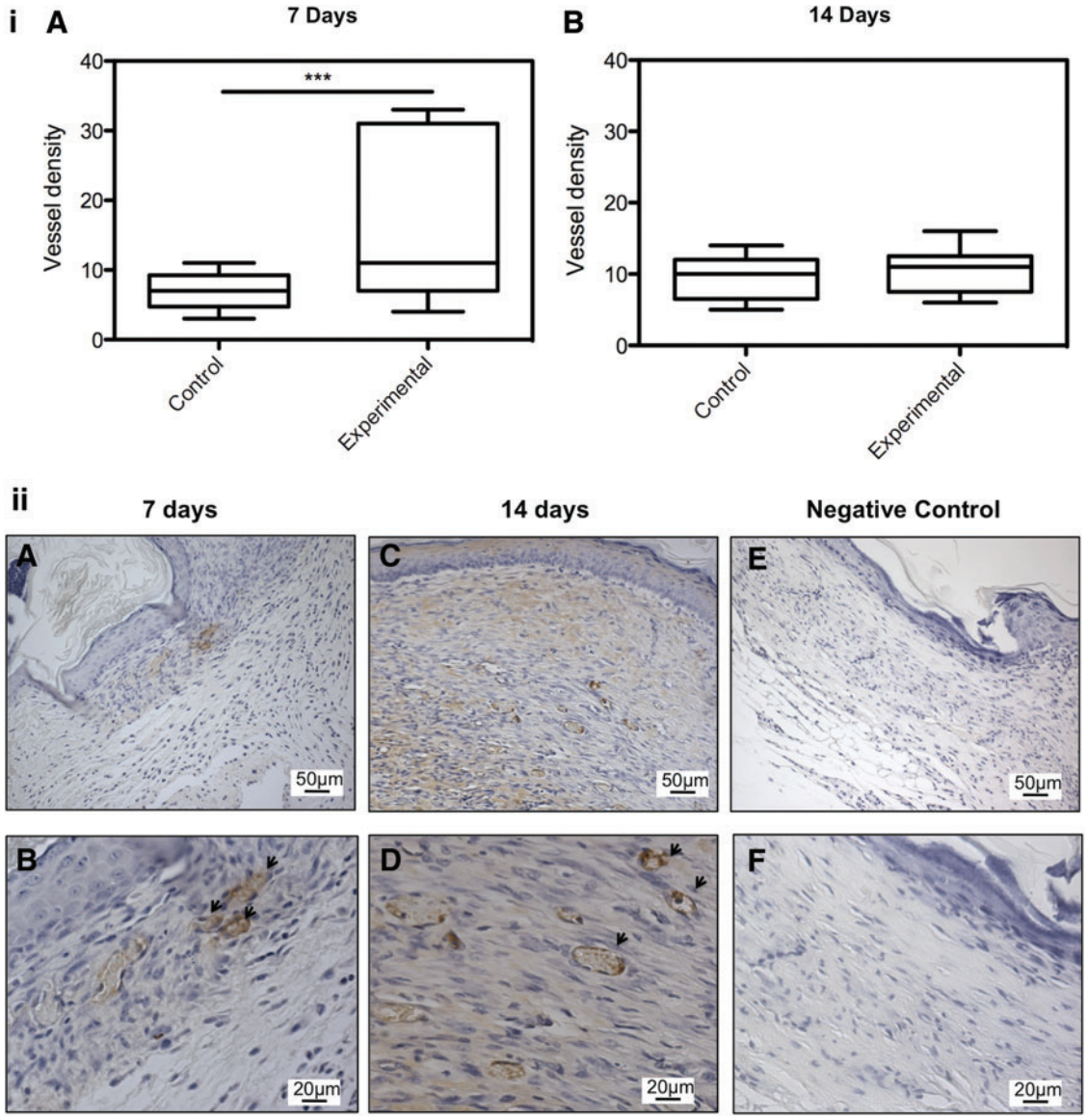

FIG. 6. Neovascularization effect of the proposed spongy-like hydrogel construct. **(i)** Graphical representation of the vessel density at the wounded area after **(A)** 7 days and **(B)** 14 days of implantation. Quantification was performed on the vessels positive for CD31. **(ii)** Immunolocalization of human endothelial CD31-positive cells (arrows) in the experimental group after **(A, B)** 7 days and **(C, D)** 14 days postoperative. **(B, D,** and **F)** Represent higher magnification images of **(A, C, E)**, respectively. **(E, F)** Represent the immunostaining negative controls. ***$p < 0.001$. Color images available online at www.liebertpub.com/tea

tissue digestion that can be delaying the adhesion of the cells within the spongy-like hydrogels.

It is recognized that a 3D environment contributes to the cell state modulation,[37] which supports the assumption that the 3D niche, created before implantation, would facilitate a well-orchestrated wound healing process contributing to the expected outcome of our strategy and to the formation of good quality neoskin. The application of spongy-like hydrogels constructs *in vivo* resulted in significant improvements at the early stages of wound healing. Wound closure, in specific, was significantly enhanced in the first time point, in comparison to the control group, along with a more exuberant exudate formation and the infiltration of the inflammatory cells into the spongy-like hydrogels. These observations are in accordance to our previous data regarding acellular GG-HA spongy-like hydrogels implantation in a similar model that also showed that this superior exudate absorption capacity contributed to the spongy-like hydrogel rapid degradation.[38] As granulation tissue is a transient template, rich in fibrin, fibronectin, collagen type I and III, and also hyaluronan,[39] determinant for the neoepidermis morphogenesis and neotissue deposition,[40] its dynamics of growth and remodeling is one of the most relevant aspects of wound healing. The rationale of using HA in the spongy-like hydrogel composition was to provide an additional, although also temporary, supporting framework within the wound bed for the integration of transplanted cells. HA has been increasingly studied to direct and control neovascularization of tissue constructs *in vitro* or *in vivo*.[41] However, the biological roles and cellular interactions of

HA with cells are HA chain length-dependent. While long-chain HA serves to maintain a highly hydrated environment and regulate osmotic balance, acting as a lubricant,[33,41] small HA oligomers induce inflammatory cytokine release by inflammatory cells, which then modulate later wound healing phases cascade of events.[32–36,42] The transplanted human cells were detected at early time points, not only inside the spongy-like hydrogel but also in the neotissue forming underneath, suggesting their contribution to wound closure. Moreover, wounds treated with spongy-like hydrogel constructs showed improved neovascularization at early time points. After 7 days, the number of vessels present in the wounded area was significantly higher in the experimental condition than in the controls, and more importantly, human-derived and chimeric vessels were detected at days 7 and 14, showing the direct contribution of the transplanted endothelial cells.

Despite the observed results regarding the enhanced effect over wound closure, re-epithelialization, hair-follicle formation, and neovascularization/angiogenesis in the presence of the GG-HA spongy-like hydrogels, the hypothesis herein proposed of using this as a template to induce self-organization of human skin cells, turned out to be unrealistic. In fact, the human transplanted cells were only detected at early time points; therefore, we consider that GG-HA spongy-like hydrogel failed in providing an adequate framework for that purpose. The rapid degradation of the implanted constructs, as described in our previous work,[38] did not allow to fully take advantage of the type of cells within both the epidermal and dermal fractions and of the multiple communication routes known to occur between them.[43] Nonetheless, our observations meet the intermediate formation of epidermis and later hair follicle detection, as observed by Lee *et al.*,[13] but, in addition to the use of newborn mice cells instead of human cells, no data regarding the origin of the organized structures formed were reported.

Thus, the herein proposed approach failed in providing the necessary conditions to allow dissociated human epidermal and dermal cellular fractions to self-organize along the wound healing process. Nonetheless, the GG-HA spongy-like hydrogel acted as a suitable supporting matrix for the transplanted cells during the early time points allowing them to contribute to the observed early wounds re-epithelialization and neovascularization.

Our strategy proposes a combination of a GG-HA spongy-like hydrogel and freshly dissociated skin relevant lineages for the promotion of cells self-organization *in vivo*. The generated construct was able to accelerate the wound healing process, successfully promoting earlier re-epithelialization, increased formation of hair follicle appendages, and an overall enhanced re-vascularization at early time points that assured the nourishment of neoformed tissue. However, this system did not sustain the hypothesized self-organization of entrapped cells, possibly due to the suggested rapid degradation.

Acknowledgments

We thank the Hospital da Prelada (Porto), in particular Dr. Paulo Costa for lipoaspirates collection and to financial support by Skingineering (PTDC/SAU-OSM/099422/2008), Portuguese Foundation for Science and Technology (FCT)-funded project. The research leading to these results has also received funding from the European Union's Seventh Framework Programme (FP7/2007–2013) under grant agreement no. REGPOT-CT2012-316331-POLARIS.

Disclosure Statement

No competing financial interests exist.

References

1. Schiestl, C., Stiefel, D., and Meuli, M. Giant naevus, giant excision, eleg(i)ant closure? Reconstructive surgery with Integra Artificial Skin to treat giant congenital melanocytic naevi in children. J Plast Reconstr Aesthet Surg **63,** 610, 2009.
2. Haslik, W., Kamolz, L.P., Nathschlager, G., Andel, H., Meissl, G., and Frey, M. First experiences with the collagen-elastin matrix Matriderm as a dermal substitute in severe burn injuries of the hand. Burns **33,** 364, 2007.
3. Waymack, P., Duff, R.G., and Sabolinski, M. The effect of a tissue engineered bilayered living skin analog, over meshed split-thickness autografts on the healing of excised burn wounds. The Apligraf Burn Study Group. Burns **26,** 609, 2000.
4. Marston, W.A., Hanft, J., Norwood, P., and Pollak, R. The efficacy and safety of Dermagraft in improving the healing of chronic diabetic foot ulcers: results of a prospective randomized trial. Diabetes Care **26,** 1701, 2003.
5. Butler, C.E., and Orgill, D.P. Simultaneous *in vivo* regeneration of neodermis, epidermis, and basement membrane. Adv Biochem Eng Biotechnol **94,** 23, 2005.
6. Supp, D.M., and Boyce, S.T. Engineered skin substitutes: practices and potentials. Clin Dermatol **23,** 403, 2005.
7. Supp, D.M., Wilson-Landy, K., and Boyce, S.T. Human dermal microvascular endothelial cells form vascular analogs in cultured skin substitutes after grafting to athymic mice. FASEB J **16,** 797, 2002.
8. Bottcher-Haberzeth, S., Biedermann, T., and Reichmann, E. Tissue engineering of skin. Burns **36,** 450, 2009.
9. Enoch, S., Roshan, A., and Shah, M. Emergency and early management of burns and scalds. BMJ **338,** b1037, 2009.
10. Horch, R.E., Kopp, J., Kneser, U., Beier, J., and Bach, A.D. Tissue engineering of cultured skin substitutes. J Cell Mol Med **9,** 592, 2005.
11. Gurtner, G.C., Werner, S., Barrandon, Y., and Longaker, M.T. Wound repair and regeneration. Nature **453,** 314, 2008.
12. Aarabi, S., Longaker, M.T., and Gurtner, G.C. Hypertrophic scar formation following burns and trauma: new approaches to treatment. PLoS Med **4,** e234, 2007.
13. Lee, L.F., Jiang, T.X., Garner, W., and Chuong, C.M. A simplified procedure to reconstitute hair-producing skin. Tissue Eng Part C Methods **17,** 391, 2010.
14. Sun, T., Mai, S., Norton, D., Haycock, J.W., Ryan, A.J., and MacNeil, S. Self-organization of skin cells in three-dimensional electrospun polystyrene scaffolds. Tissue Eng **11,** 1023, 2005.
15. Delvoye, P., Pierard, D., Noel, A., Nusgens, B., Foidart, J.M., and Lapiere, C.M. Fibroblasts induce the assembly of the macromolecules of the basement membrane. J Invest Dermatol **90,** 276, 1988.
16. Konig, A., and Bruckner-Tuderman, L. Epithelial-mesenchymal interactions enhance expression of collagen VII *in vitro*. J Invest Dermatol **96,** 803, 1991.

17. Havlickova, B., Biro, T., Mescalchin, A., Tschirschmann, M., Mollenkopf, H., Bettermann, A., *et al.* A human folliculoid microsphere assay for exploring epithelial- mesenchymal interactions in the human hair follicle. J Invest Dermatol **129,** 972, 2009.
18. Ahmed, T.A., Dare, E.V., and Hincke, M. Fibrin: a versatile scaffold for tissue engineering applications. Tissue Eng Part B Rev **14,** 199, 2008.
19. Sanders, J.E., Stiles, C.E., and Hayes, C.L. Tissue response to single-polymer fibers of varying diameters: evaluation of fibrous encapsulation and macrophage density. J Biomed Mater Res **52,** 231, 2000.
20. Ng, K.W., Hutmacher, D.W., Schantz, J.T., Ng, C.S., Too, H.P., Lim, T.C., *et al.* Evaluation of ultra-thin poly(epsilon-caprolactone) films for tissue-engineered skin. Tissue Eng **7,** 441, 2001.
21. van Dorp, A.G., Verhoeven, M.C., Koerten, H.K., van Blitterswijk, C.A., and Ponec, M. Bilayered biodegradable poly(ethylene glycol)/poly(butylene terephthalate) copolymer (Polyactive) as substrate for human fibroblasts and keratinocytes. J Biomed Mater Res **47,** 292, 1999.
22. Wong, V.W., Rustad, K.C., Galvez, M.G., Neofytou, E., Glotzbach, J.P., Januszyk, M., *et al.* Engineered pullulan-collagen composite dermal hydrogels improve early cutaneous wound healing. Tissue Eng Part A **17,** 631, 2010.
23. Tran, N.Q., Joung, Y.K., Lih, E., and Park, K.D. *In situ* forming and rutin-releasing chitosan hydrogels as injectable dressings for dermal wound healing. Biomacromolecules **12,** 2872, 2011.
24. Sun, G., Zhang, X., Shen, Y.I., Sebastian, R., Dickinson, L.E., Fox-Talbot, K., *et al.* Dextran hydrogel scaffolds enhance angiogenic responses and promote complete skin regeneration during burn wound healing. Proc Natl Acad Sci U S A **108,** 20976, 2011.
25. Luo, Y., Diao, H., Xia, S., Dong, L., Chen, J., and Zhang, J. A physiologically active polysaccharide hydrogel promotes wound healing. J Biomed Mater Res A **94,** 193, 2010.
26. Khademhosseini, A., and Langer, R. Microengineered hydrogels for tissue engineering. Biomaterials **28,** 5087, 2007.
27. da Silva, L.C., Cerqueira, M.T., Marques, A.P., Correlo, V.M., Sousa, R.A., and Reis, R.L. Gellan Gum-based spongy-like hydrogels: methods and biomedical applications thereof. Portugal. Provisional Patent 106890. 2013.
28. Oliveira, J.T., Martins, L., Picciochi, R., Malafaya, P.B., Sousa, R.A., Neves, N.M., *et al.* Gellan gum: a new biomaterial for cartilage tissue engineering applications. J Biomed Mater Res A **93,** 852, 2009.
29. Wicke, C., Halliday, B., Allen, D., Roche, N.S., Scheuenstuhl, H., Spencer, M.M., *et al.* Effects of steroids and retinoids on wound healing. Arch Surg **135,** 1265, 2000.
30. Ananta, M., Brown, R.A., and Mudera, V. A rapid fabricated living dermal equivalent for skin tissue engineering: an *in vivo* evaluation in an acute wound model. Tissue Eng Part A **18,** 353, 2011.
31. Liu, S., Zhang, H., Zhang, X., Lu, W., Huang, X., Xie, H., *et al.* Synergistic angiogenesis promoting effects of extracellular matrix scaffolds and adipose-derived stem cells during wound repair. Tissue Eng Part A **17,** 725, 2011.
32. Price, R.D., Myers, S., Leigh, I.M., and Navsaria, H.A. The role of hyaluronic acid in wound healing: assessment of clinical evidence. Am J Clin Dermatol **6,** 393, 2005.
33. Kirker, K.R., Luo, Y., Nielson, J.H., Shelby, J., and Prestwich, G.D. Glycosaminoglycan hydrogel films as bio-interactive dressings for wound healing. Biomaterials **23,** 3661, 2002.
34. Tonello, C., Vindigni, V., Zavan, B., Abatangelo, S., Abatangelo, G., Brun, P., *et al. In vitro* reconstruction of an endothelialized skin substitute provided with a microcapillary network using biopolymer scaffolds. FASEB J **19,** 1546, 2005.
35. Gao, F., Liu, Y., He, Y., Yang, C., Wang, Y., Shi, X., *et al.* Hyaluronan oligosaccharides promote excisional wound healing through enhanced angiogenesis. Matrix Biol **29,** 107, 2010.
36. Ibrahim, S., and Ramamurthi, A. Hyaluronic acid cues for functional endothelialization of vascular constructs. J Tissue Eng Regen Med **2,** 22, 2008.
37. Green, J.A., and Yamada, K.M. Three-dimensional microenvironments modulate fibroblast signaling responses. Adv Drug Deliv Rev **59,** 1293, 2007.
38. Cerqueira, M., da Silva, L.P., Santos, T.C., Pirraco, R.P., Martins, A.R., Correlo, V.M., Marques, A.P., and Reis, R.L. Pre-vascularized Gellan Gum-Hyaluronic Acid Spongy-like Hydrogels improve Skin wound healing. Presented at the Annual Meeting of the Society For Biomaterials 2013, Boston, USA.
39. Witte, M.B., and Barbul, A. General principles of wound healing. Surg Clin North Am **77,** 509, 1997.
40. Singer, A.J., and Clark, R.A. Cutaneous wound healing. N Engl J Med **341,** 738, 1999.
41. Pardue, E.L., Ibrahim, S., and Ramamurthi, A. Role of hyaluronan in angiogenesis and its utility to angiogenic tissue engineering. Organogenesis **4,** 203, 2008.
42. Noble, P.W. Hyaluronan and its catabolic products in tissue injury and repair. Matrix Biol **21,** 25, 2002.
43. Lugo, L.M., Lei, P., and Andreadis, S.T. Vascularization of the dermal support enhances wound re-epithelialization by *in situ* delivery of epidermal keratinocytes. Tissue Eng Part A **17,** 665, 2010.

Address correspondence to:
Alexandra P. Marques, PhD
3B's Research Group—Biomaterials, Biodegradables and Biomimetics
University of Minho
Headquarters of the European Institute of Excellence on Tissue Engineering and Regenerative Medicine
AvePark
Zona Industrial da Gandra
S. Cláudio do Barco
4806-909 Caldas das Taipas
Guimarães
Portugal

E-mail: apmarques@dep.uminho.pt

Received: July 26, 2013
Accepted: November 25, 2013
Online Publication Date: January 16, 2014